



저작자표시 2.0 대한민국

이용자는 아래의 조건을 따르는 경우에 한하여 자유롭게

- 이 저작물을 복제, 배포, 전송, 전시, 공연 및 방송할 수 있습니다.
- 이차적 저작물을 작성할 수 있습니다.
- 이 저작물을 영리 목적으로 이용할 수 있습니다.

다음과 같은 조건을 따라야 합니다:



저작자표시. 귀하는 원저작자를 표시하여야 합니다.

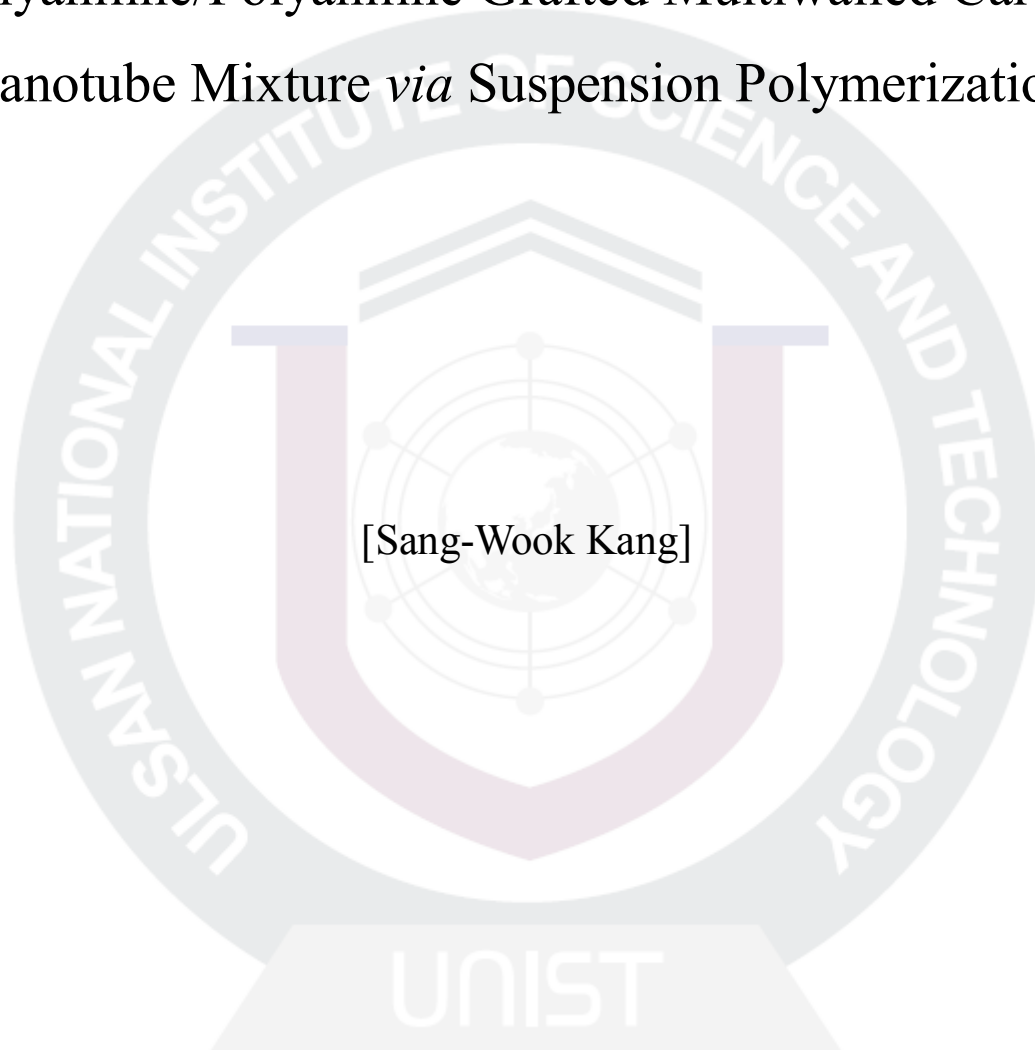
- 귀하는, 이 저작물의 재이용이나 배포의 경우, 이 저작물에 적용된 이용허락조건을 명확하게 나타내어야 합니다.
- 저작권자로부터 별도의 허가를 받으면 이러한 조건들은 적용되지 않습니다.

저작권법에 따른 이용자의 권리는 위의 내용에 의하여 영향을 받지 않습니다.

이것은 [이용허락규약\(Legal Code\)](#)을 이해하기 쉽게 요약한 것입니다.

[Disclaimer](#) 

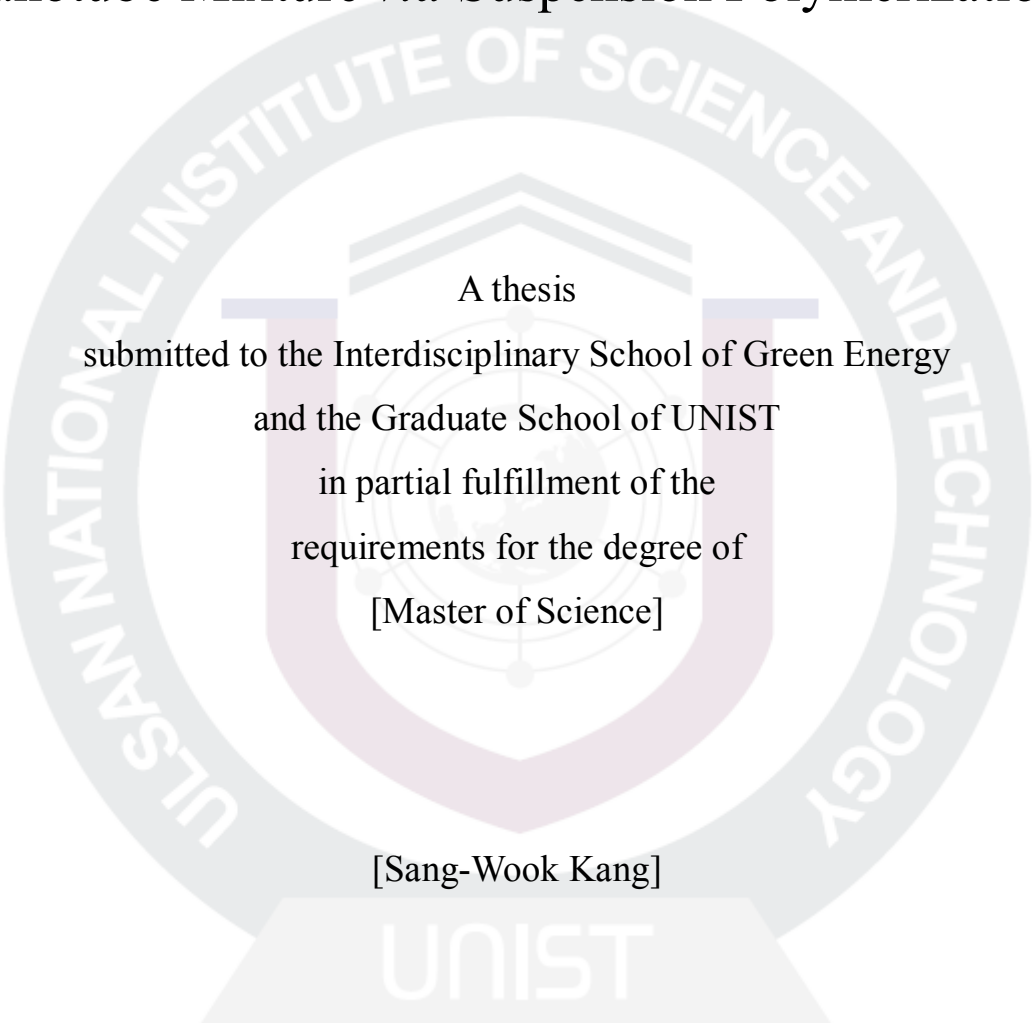
[Synthesis and Electrical Properties of
Polyaniline/Polyaniline Grafted Multiwalled Carbon
Nanotube Mixture *via* Suspension Polymerization]



[Sang-Wook Kang]

[Interdisciplinary School of Green Energy]
Graduate School of UNIST

[Synthesis and Electrical Properties of
Polyaniline/Polyaniline Grafted Multiwalled Carbon
Nanotube Mixture *via* Suspension Polymerization]



A thesis
submitted to the Interdisciplinary School of Green Energy
and the Graduate School of UNIST
in partial fulfillment of the
requirements for the degree of
[Master of Science]

[Sang-Wook Kang]

05. 28. 2010

Approved by

Major Advisor
[Jong-Beom, Baek]

[Synthesis and Electrical Properties of
Polyaniline/Polyaniline Grafted Multiwalled Carbon
Nanotube Mixture *via* Suspension Polymerization]

[Sang-Wook Kang]

This certifies that the thesis of [Sang-Wook Kang] is approved.

05. 28. 2010

[signature]

Thesis supervisor: [Jong-Beom, Baek]

[signature]

[Byeong-Su, Kim]

[signature]

[Hyeon-Suk, Shin]

Abstract

The mixture of polyaniline (PANI) and PANi-grafted multiwalled carbon nanotube (PANI/PANi-g-MWNT mixture) was prepared by suspension polymerization. MWNT was first functionalized with 4-aminobenzoic acid via “direct” Friedel-Crafts acylation in polyphosphoric acid (PPA)/phosphorous pentoxide (P_2O_5) medium to afford 4-aminobenzoyl-functionalized MWNT (AF-MWNT). The resulting 4-aminobenzoyl-functionalized multiwalled carbon nanotube was then treated with aniline in the presence of ammonium persulfate/aqueous hydrochloric acid to promote a suspension polymerization. The resultant composite was characterized by elemental analysis, Fourier-transform infrared spectroscopy, wide angle x-ray diffraction, scanning electron microscopy, transmission electron microscopy, UV-vis absorption spectroscopy, fluorescence spectroscopy, cyclic voltammetry, and electrical conductivity measurement. The electrical conductivity of polyaniline grafted multiwalled carbon nanotube composite was improved compared to that of polyaniline control. Specifically, the electrical conductivity of polyaniline grafted multiwalled carbon nanotube was improved 1.5~3500 times depending upon the level of doping of what. The capacitance of the composite was also greatly enhanced.

Contents

I . Introduction-----	1
II. Experiment-----	3
2.1 Materials-----	3
2.2 Instrumentations-----	3
2.3 Functionalization of MWNT-----	3
2.4 Suspension polymerization of PANi homopolymer-----	4
2.5 Suspension polymerization of PANi/PANi-g-MWNT mixture-----	4
2.6 Further Purification (Partial Dedoping) of PANi and PANi/PANi-g-MWNT mixture -----	5
2.7 Dedoping of PANi and PANi-g-MWNT mixture -----	5
2.8 Doping of PANi and PANi-g-MWNT mixture -----	5
III. Results and discussion-----	6
3.1 Functionalization of MWNT-----	6
3.2 FT-IR study-----	8
3.3 Wide-angle X-ray diffraction (WAXD) -----	9
3.4 Scanning electron microscopy-----	10
3.5 Transmission electron microscopy-----	11
3.6 BET surface area-----	12
3.7 UV-vis absorption and emission behaviors-----	13
3.8 Cyclic voltammetry-----	14
3.9 Electrical characteristics-----	15
IV. Conclusions-----	17
References-----	18
Appendix-----	24
Manuscript-----	27
Acknowledgements-----	28

List of figures

Figure 1. FT-IR (KBr pellet) spectra of PANi and PANi/PANi-g-MWNT mixture.

Figure 2. WAXD patterns: (a) PANi, (b) PANi/PANi-g-MWNT mixture.

Figure 3. SEM images: (a) PANi (30,000×), (b) PANi (100,000×), (c) PANi/PANi-g-MWNT mixture (30,000×), (d) PANi/PANi-g-MWNT mixture (100,000×).

Figure 4. TEM images: (a) PANi (30,000×), (b) PANi (150,000×), (c) PANi/PANi-g-MWNT mixture (300,000×), (d) PANi/PANi-g-MWNT mixture (500,000×).

Figure 5. UV-vis absorption and emission spectra of PANi and PANi/PANi-g-MWNT mixture: (a) absorption, (b) emission.

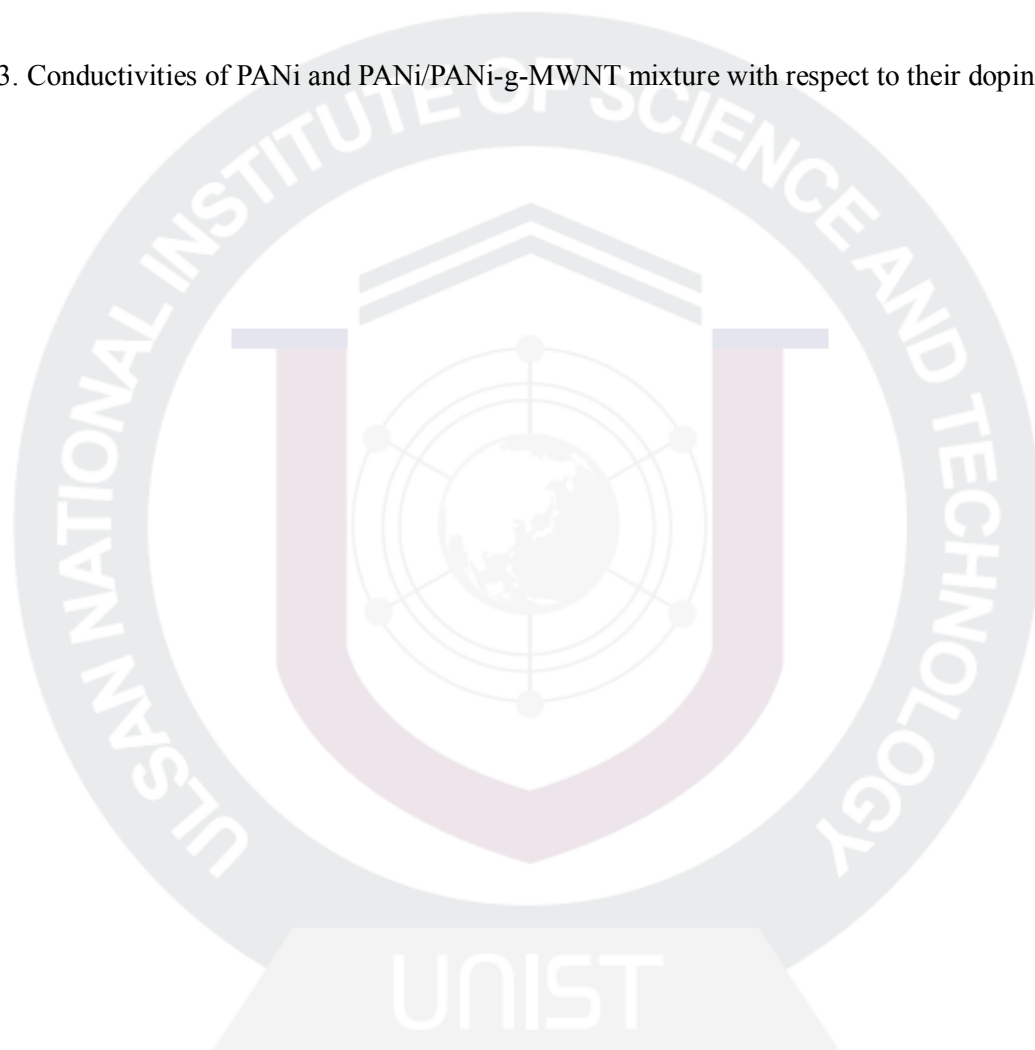
Figure 6. Cyclic voltammograms of PANi and PANi/PANi-g-MWNT mixture in 0.1M H₂SO₄ aqueous solution. Scan rate is 10mV/s (black line) PANi, (red line) PANi/PANi-g-MWNT mixture.

List of tables

Table 1. Elemental analysis of samples.

Table 2. BET surface area, pore volume and average pore size of PANi and PANi/PANi-g-MWNT mixture.

Table 3. Conductivities of PANi and PANi/PANi-g-MWNT mixture with respect to their doping state.



List of Schemes

Scheme 1. (a) Functionalization of MWNT in PPA/P₂O₅, (b) grafting of PANi onto the surface of AF-MWNT in HCl (1M)/CH₂Cl₂, (c) polymerization of aniline in HCl(1M)/CH₂Cl₂. The structure for functionalized and PANi/PANi-g-MWNT mixture is idealized for easy visualization of the concept present here.



Nomenclature

PANi	polyaniline
CNT	Carbon Nanotube
MWNT	Multiwalled Carbon Nanotube
F-CNT	functionalized CNT
PPA	polyphosphoric acid
P₂O₅	phosphorous pentoxide
NMP	N-methyl-2-pyrrolidone
AF-MWNT	4-aminobenzoyl-functionalized MWNT
PANi-g-MWNT	PANi grafted MWNT
HCl	hydrochloric acid
APS	ammonium persulfate
CH₂Cl₂	dichloromethane
NH₄OH	ammonium hydroxide
FT-IR	Fourier transform spectroscopy
WAXD	Wide-angle X-ray diffraction
SEM	Scanning electron microscopy
TEM	Transmission electron microscopy
BET	Brunauer-Emmett-Teller
UV	ultraviolet
CV	cyclic voltammetry
EA	elemental analyses

I. Introduction

Doping of polyacetylene with iodine increases its electrical conductivity of 10^8 times. The phenomenon has been discovered in 1977.¹ Since then, conducting polymers including polyacetylene have been attracted a lot of interest for a variety of applications. However, polyacetylene is easily oxidized in air due to poor stability. As a result, its study has remained just as an academic legacy. The researches on conducting polymers were actively backed on track by Macdiarmid and Heeger after finding polyaniline (PANi) as a stable conducting polymer upon doping.² PANi has been appreciated by various fields of applications and it is a strong candidate amongst other conducting polymers. As a result of various studies of molecular structure and conduction mechanism, PANi has been considered to display good electronic, thermoelectric, and optical properties as well as environmental stability.³ In addition, its doping level can be readily controlled through an acid doping-base dedoping processes. It also has a wide range of electrical properties which can be easily controlled by changing its oxidation and protonation states.⁴ It has been used for many applications such as organic lightweight batteries,⁵ microelectronics,⁶ electrorheological fluids,⁷ chemical sensors,⁸ separation membranes,⁹ and antistatic coatings.¹⁰

Carbon nanotubes (CNT) have been anticipated inventing a new class of advanced materials due to their unique structural, mechanical and electrical properties.¹¹ Recent studies have shown that the formation of polymer/CNT composites is considered as a viable approach for a manufacturing of CNT into polymer-based devices.¹² Many polymers have been used as matrix materials in polymer/CNT composites for various targeted applications.¹³ Among these polymer/CNT composites, many reports have focused on the combination of CNT and conducting polymers including poly(3-ethylenedioxythiophene)/CNT,¹⁴ poly(3-octylthiophene)/CNT,¹⁵ and poly(*p*-phenylene vinylene)/CNT.¹⁶ The resultant polymer/CNT composites have been proposed for a wide range of applications, including an amperometric biosensor for DNA¹⁷ and choline,¹⁸ a sensor for nitrogen oxide,¹⁹ and a contact in plastic electronics.²⁰ Since the hybridization of PANi and CNT could be expected to be more promising materials, many reports on PANi/CNT systems have been reported for opto-electronic and sensor applications.²¹ In order to achieve maximum enhanced properties from resultant composites, two important issues have to be resolved first. The one is the homogeneous dispersion of CNT, to provide maximum surface interactions between polymer and CNT interfaces, hitherto, harsh chemical treatments in strong acids such as sulfuric acid, nitric acid or their mixture, and/or physical treatments such as sonication have been commonly applied.²² Unfortunately, these approaches often result in significant damages to the CNT framework, which involve sidewall opening, breaking, and turning into amorphous carbon.²³ The damage on CNT would definitely weaken their original outstanding original properties such as electrical and physical properties.²⁴ In

addition to the damage issue, the other is strong interfacial adhesion between polymer and CNT, which is a prerequisite to efficiently transfer the properties of CNT into the supporting polymer matrix. However, most of previous approaches involve that CNT is physically dispersed in conducting polymer matrices with secondary interaction such as van der Waals attraction, which may not be strong enough for the ultimate transfer of CNT properties. Thus, covalent links between CNT and polymer matrix would be a better option.

As our initial attempt on the area of CNT chemistry, the less destructive chemical modification of various carbon nanomaterials via electrophilic substitution reaction in a mild polyphosphoric acid (PPA)/phosphorous pentoxide (P_2O_5) medium has been developed.^{2 5} It is a so-called “direct” Friedel-Crafts acylation reaction, which is advantageous over conventional Friedel-Crafts acylation because most of substituted benzoic acids can be used instead of corrosive and less commercially available benzoyl chlorides. Although there is little or no structural damage to the functionalized CNT (F-CNT) in PPA/ P_2O_5 medium, the covalent attachment of organics onto the sidewall of CNT could still disintegrate the electronic continuum on the surface of CNT. As a result, their electrical and thermal conductivities could be somewhat sacrificed. To compensate the loss, the covalent grafting of conducting polymer onto the surface of F-CNT could be a viable approach to minimize diminution of the electrical conductivity. Considering the ample precedents, we have demonstrated previously that the grafting of poly (phenylene sulfide) onto the surface of 4-chlorobenzoyl-functionalized MWNT enhances the electrical conductivity of the resultant composite.^{2 6} An efficient approach for the hybridization of the most commodity conducting polymer PANi and CNT is an important challenge.

Herein, we report the preparation of 4-aminobenzoyl-functionalized multiwalled carbon nanotube (AF-MWNT) and grafting of PANi onto the surface of AF-MWNT to afford PANi grafted MWNT composite (PANi/PANi-g-MWNT mixture). AF-MWNT with reactive aromatic amine groups, where PANi could be “grafted from”, was prepared via the reaction between the 4-aminobenzoic acid and MWNT in the mild PPA/ P_2O_5 medium. A subsequent suspension polymerization between aniline as monomer and AF-MWNT was conducted in ammonium persulfate (APS)/1 M aqueous hydrochloric acid (HCl) to yield PANi/PANi-g-MWNT mixture. The resultant composite was expected to show improved conductivity compared to control PANi homopolymer without MWNT.

II. Experiment

2.1 Materials

All reagents and solvents were purchased from Aldrich Chemical Inc. and Lancaster Synthesis Inc. and used as received, unless otherwise specified. MWNT (CVD MWNT 95 with diameter of ~20 nm and length of 10-50 μm) was obtained from Hanhwa Nanotech Co., LTD, Seoul, Korea.

2.2 Instrumentations

Infrared (IR) spectra were recorded on PerkinElmer spectrum 100 FT-IR spectrometer. Solid samples were embedded in KBr disks. Elemental analyses (EA) were performed with a CE Instruments EA1110. The field emission scanning electron microscopy (FE-SEM) used in this work was done using LEO 1530FE and NanoSem 230. The field emission transmission electron microscopy (FE-TEM) was done using a FEI Tecnai G2 F30 S-Twin. The Brunauer-Emmett-Teller (BET) surface area was measured by nitrogen adsorption-desorption isotherms using Micromeritics ASAP 2504N. Wide-angle X-ray diffraction (WAXD) powder patterns were recorded with a Rigaku RU-200 diffractometer using Ni-filtered Cu K α radiation (40 kV, 100 mA, $\lambda = 0.15418$ nm). UV-vis spectra were obtained on a Varian Cary 5000 UV-vis spectrometer. Stock solutions were prepared by dissolving 10 mg of each sample in 1 L of *N*-methyl-2-pyrrolidone (NMP). Photoluminescence measurements were performed with a Varian Cary Eclipse Fluorescence spectrometer. The excitation wavelength was that of the UV absorption maximum of each sample. Cyclic voltammetry (CV) experiments were performed with a 1287A Potentiostat Galvanostat Cell Test System (Solartron Analytical Ltd., UK). The test electrodes were prepared by dipping glassy carbon sheet into sample solution in NMP and the electrode was dried and used as working electrode. The CV experiment was conducted in 1.0M aqueous sulfuric acid solution with a scan rate of 10 mV/s and in the potential of -0.25 and 1.25 V. The three-electrode system consisted of a carbon cloth electrode as working electrode, an Ag/AgCl (sat. KCl) as reference electrode and platinum gauze as counter electrode. All potential values are reported as a function of Ag/AgCl. The surface conductivity (surface resistance) of samples was measured at room temperature by four-point probe method using Advanced Instrument Technology (AIT) CMT-SR1000N with Jandel Engineering probe. The reported conductivity values are averages of 10 measurements.

2.3 Functionalization of MWNT

Into a resin flask equipped with high torque mechanical stirrer, nitrogen inlet and outlet, 4-aminobenzoic acid (10.0g, 73 mmol), MWNT (5.0 g), PPA (300.0 g, 83% P₂O₅ assay) and P₂O₅ (75.0 g) were placed. The flask was immersed in oil bath and gently heated to 100 °C. The reaction mixture was stirred at the temperature for 1h. The reaction mixture was then heated to 130 °C and stirred for 72h under nitrogen atmosphere. The dark homogeneous mixture was poured into water. The precipitates were collected by suction filtration and Soxhlet extracted with distilled water for three days and methanol for three days, and finally freeze dried for 48h to yield 9.82g (71.7% yield) of dark black powder. Anal. Calcd. for C_{12.71}H₆O₁N₁: C, 80.89%; H, 3.21%; N, 7.42%. Found: C, 79.06%; H, 2.20%; N, 5.45%.

2.4 Suspension Polymerization of PANi homopolymer

In a 250ml three-necked, round-bottom flask with magnetic stirring bar, CH₂Cl₂(50ml), H₂O (100 ml) and then was stirred at 200 rpm for 30 min. 25 mL of 1M HCl solution containing aniline (10.0 g, 0.107 mol) was added into the solution and stirred for 1h. 1M HCl (25mL) solution containing APS (6.2 g, 0.027 mol) was added in one portion into the solution. The reaction mixture was stirred for additional 6h at room temperature. The reactant color changed from lime-green to dark-green. The dark green precipitate was collected by suction filtration, washed with distilled water and methanol and finally freeze dried under reduced pressure for 48h to give 1.68g (16.8% yield) of dark green PANi powder. Found: C, 60.34%; H, 5.23%; N, 12.44%. Since the level of HCl doping was unknown, the yield and theoretical carbon-hydrogen-nitrogen (CHN) contents could not be precisely calculated.

2.5 Suspension Polymerization of PANi/PANi-g-MWNT

Two solutions were independently prepared in different flask. The one is a solution containing aniline (9 g, 0.963 mol) in CH₂Cl₂ (25 mL), AF-MWNT (1.0 g) was dispersed with ultrasonication for 5min. The other is a solution containing APS (6.2 g, 0.027 mol) in 1M HCl (25 mL). Both solutions were added in a 250 ml three-necked, round-bottom flask with magnetic stirring bar, CH₂Cl₂(50ml), H₂O (100 ml) and the reaction mixture was stirred at 200 rpm for 30min. The rest of reaction and work-up procedures were similar to those of PANi synthesis. The color of aniline/AF-MWNT/CH₂Cl₂ solution was from dark black to light brown. The resulting dark green precipitates were collected by filtration. The product was repeatedly washed with distilled water. Finally, it was freeze-dried under

reduced pressure (0.5 mmHg) for 48h to give 2.74g (27.4% yield) of dark green powder. Found: C, 64.57%; H, 4.69%; N, 10.71%. Since the level of HCl doping in PANi was unknown, the yield and theoretical CHN contents could not be precisely calculated.

2.6 Further Purification (Partial Dedoping) of PANi and PANi/PANi-g-MWNT mixture

The synthesized PANi and PANi/PANi-g-MWNT were transferred to an extraction thimble and extracted with distilled water for three days and methanol for three days, and finally freeze-dried under reduced pressure (0.5mmHg) for 48h. Found for PANi: C, 67.86%; H, 4.96%; N, 13.96%; Found for PANi/PANi-g-MWNT mixture: C, 73.30%; H, 8.31%; N, 12.01%. The yield and theoretical CHN contents could not be precisely calculated because the degree of doping was not known.

2.7 Dedoping of PANi and PANi/PANi-g-MWNT mixture

As-prepared partially doped (protonated) PANi and PANi/PANi-g-MWNT mixture were dedoped (deprotonated) by immersion of the samples into basic 1M aqueous ammonia at room temperature for 24h. Dedoped PANi and PANi/PANi-g-MWNT mixture were collected by suction filtration, washed with deionized water and finally freeze dried under reduced pressure for 48h. PANi: Anal. Calcd. for $C_6H_5N_1$: C, 79.10%; H, 5.53%; N, 15.37%. Found: C, 75.07%; H, 4.61%; N, 15.58%. PANi-g-MWCNT: Anal. Calcd. for $C_{23.15}H_{14.7}O_1N_{14.07}$: C, 80.07%; H, 4.27%; N, 11.05%. Found: C, 77.15%; H, 4.06%; N, 13.26%.

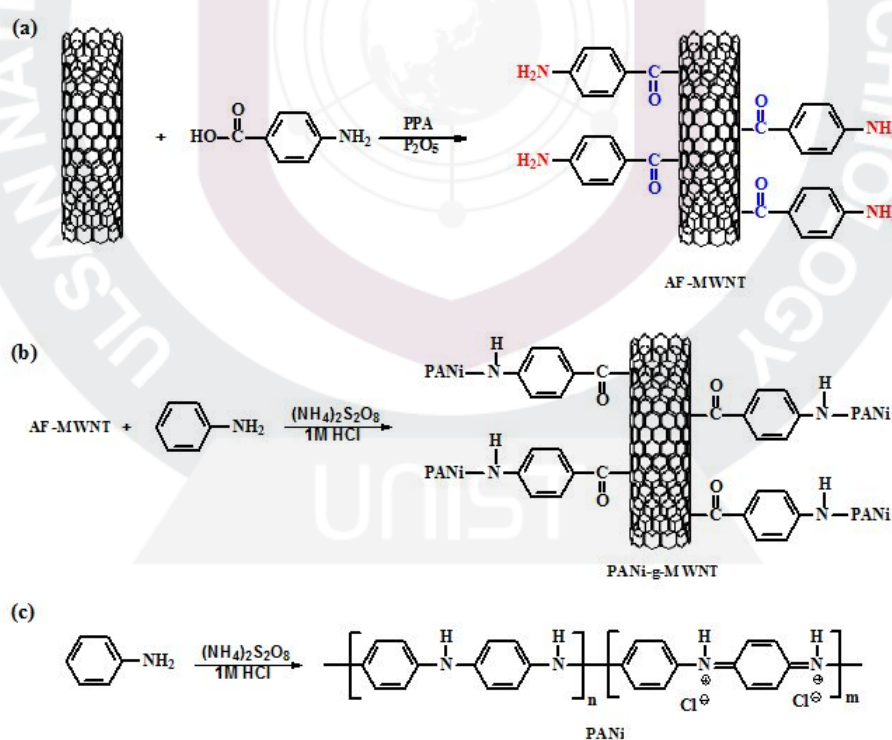
2.8 Redoping of PANi and PANi/PANi-g-MWNT mixture

The dedoped PANi and PANi/PANi-g-MWNT mixture samples were redoped (protonated) by immersion in 1M HCl at room temperature for 48h. The work-up procedure was the same as dedoping of PANi and PANi/PANi-g-MWNT mixture. Found for PANi: C, 61.41%; H, 5.07%; N, 12.84%; Found for PANi/PANi-g-MWNT mixture: C, 68.87%; H, 4.30%; N, 11.53%. The yield and theoretical CHN contents could not be precisely calculated because the degree of doping was not known.

III. Results and discussion

3.1 Functionalization of MWNT

As explained in the literature procedure,^{2,7} the functionalization of MWNT was carried out with 4-aminobenzoic acid in PPA/P₂O₅ medium at 130 °C (Scheme 1a). The resultant AF-MWNT has 4-aminobenzoyl moieties on its periphery, which could be reactive sites to present for grafting PANi *via* suspension polymerization. The CHN contents of AF-MWNT from elemental analysis (EA; see supplementary information for detailed calculation) and approximate theoretical values are summarized in Table 1. There are some difference between theoretical and measured values in the EA data, which could be stemmed from a number of factors such as the hygroscopic nature of these chemically modified carbon nanomaterials. Given that this type of materials is not easily quantified using destructive thermal characterization methods, the results may be overestimated the actual extent of functionalization.



Scheme 1. (a) Functionalization of MWNT in PPA/P₂O₅, (b) grafting of PANi onto the surface of AF-MWNT in HCl (1M)/CH₂Cl₂, (c) polymerization of aniline in HCl (1M)/CH₂Cl₂. The structure for functionalized and PANi/PANi-g-MWNT mixture is idealized for easy visualization

of the concept present here.

Table 1. Elemental analysis of samples.

Sample	Condition	EF ^a	FW ^b (g/mol)		C (%)	H (%)	N (%)
AF- MWNT	As-prepared	C _{12.71} H ₆ NO	188.76	Calcd.	80.89	3.21	7.42
				Found	79.06	2.20	5.45
PANi	As-prepared	NA	NA	Found	60.34	5.23	12.44
	After refine	NA	NA	Found	67.86	4.96	13.96
	Dedoped	C ₆ H ₅ N	91.11	Calcd.	79.10	5.53	15.37
				Found	75.07	4.61	15.58
Doped	NA	NA	Found	61.41	5.07	12.84	
PANi/PANi -g-MWNT mixture	As-prepared	NA	NA	Found	64.57	4.69	10.71
	After refine	NA	NA	Found	73.30	8.31	12.01
	Dedoped	C _{23.15} H _{14.7} N _{2.74} O	347.25	Calcd.	80.07	4.27	11.05
				Found	77.15	4.06	13.26
Doped	NA	NA	Found	68.87	4.30	11.53	

^a EF = Empirical formula; ^b FW = formula weight; ^c NA = not applicable.

3.2 FT-IR Study

The PANi homopolymers displayed the characteristic bands of secondary of amine (N-H) at 3237 cm^{-1} , the C=C stretching deformation of the quinoid structure at 1585 cm^{-1} , benzenoid rings at 1494 cm^{-1} and the C-N stretching band of the secondary aromatic amine at 1298 cm^{-1} (Figure 1). The PANi/PANi-g-MWNT sample displayed almost identical characteristic bands at 3162 , 1586 , 1494 and 1297 cm^{-1} . Compared to the number of PANi repeating units in PANi-g-MWNT composite, the relative population of C=O groups, which were only located at the covalent junctions between AF-MWNT and PANi, was too low to be clearly discerned.

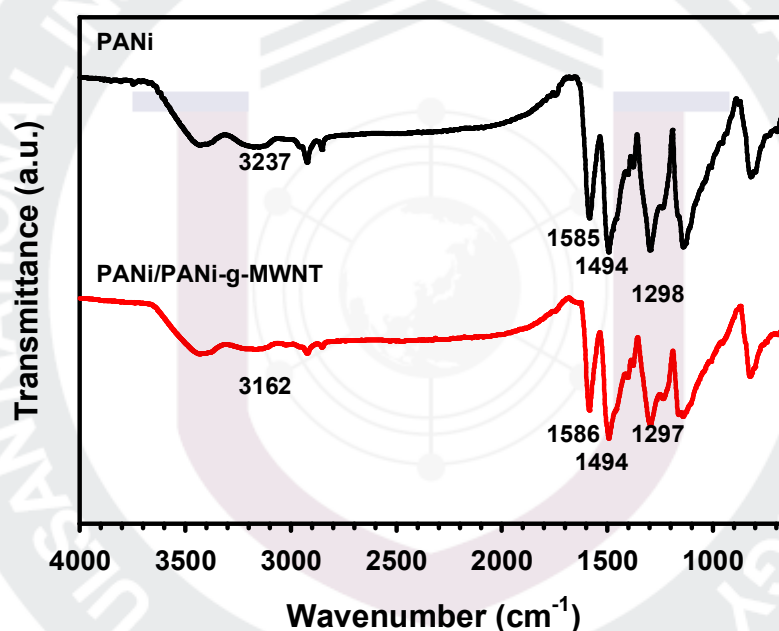


Figure 1. FT-IR (KBr pellet) spectra of PANis.

3.3 Wide-Angle x-Ray Diffraction (WAXD)

To determine the morphologies of PANi and PANi/PANi-g-MWNT mixture, as-prepared powder samples after NH_4OH dedoping were subjected to WAXD scans. The PANi showed a broad amorphous peak with relatively weak crystalline peaks at $2\theta=18.50^\circ$ (Figure 2). It indicates the major portion of PANi homopolymer is in an amorphous phase. It has been reported that the dedoped PANi as a base form exhibited different structural characteristics.²⁸ Its diffraction patterns show semicrystalline nature with one very distinct Bragg's peak at $2\theta \approx 19^\circ$. That means the dopant should affect the crystal structure and crystallinity of PANi. Therefore, although it could not be completely removed, lower crystallinity of PANi in this study implied that the HCl during the polymerization was removed during dedoping NH_4OH aqueous solution (see Experimental section).

The PANi/PANi-g-MWNT mixture displayed three strong crystalline peaks at $2\theta = 19.76, 25.62$ and 43.20° even after dedoped NH_4OH aqueous solution (Figure 2). The higher crystallinity of PANi/PANi-g-MWNT mixture than that of PANi was probably because covalently linked MWNT provided nucleation sites for PANi crystallization.

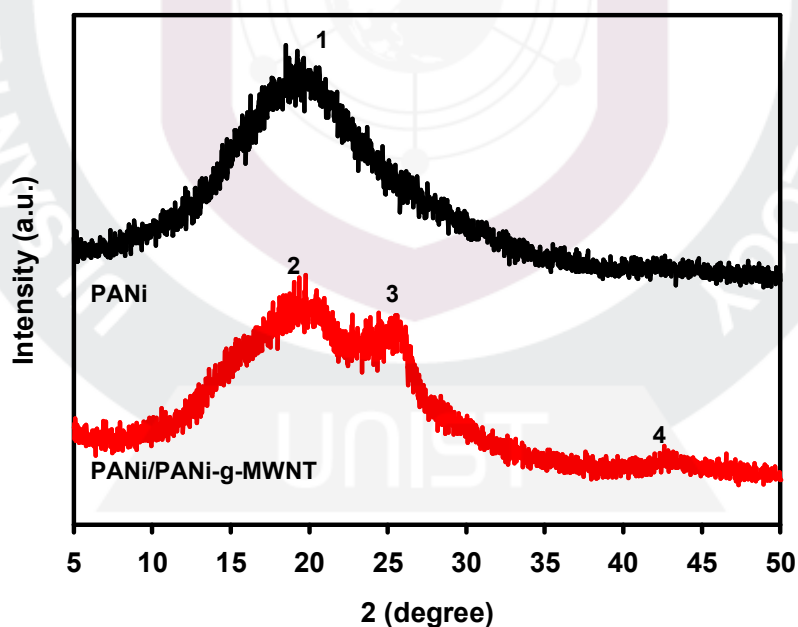


Figure 2. WAXD patterns: (top) PANi, (bottom) PANi/ PANi-g-MWNT mixture.

3.4 Scanning Electron Microscopy

Comparing the SEM images depicted in Figure 3, PANi homopolymer shows globular particles with an average diameter of 10~30 nm and covered with many protrusions (Figure 3a, b). In the case of PANi/PANi-g-MWNT mixture, nano-sized rods of PANi and nanofibers of PANi-g-MWNT are coexisted (Figure 3c, d). The average diameter of PANi-g-MWNT is approximately 80~120nm, which is larger than that of AF-MWNT, whose average diameter is 40~50nm.^{2 9} Judging from this, aniline was grafted onto the surface of AF-MWNT. Since PANi/PANi-g-MWNT mixture did not show any irregularly formed, independent particles, it can be postulated that AF-MWNT nucleation must have prevented the generation of these irregular PANi particles. The overall SEM results further support that PANi has been covalently grafted onto the surface of AF-MWNT.

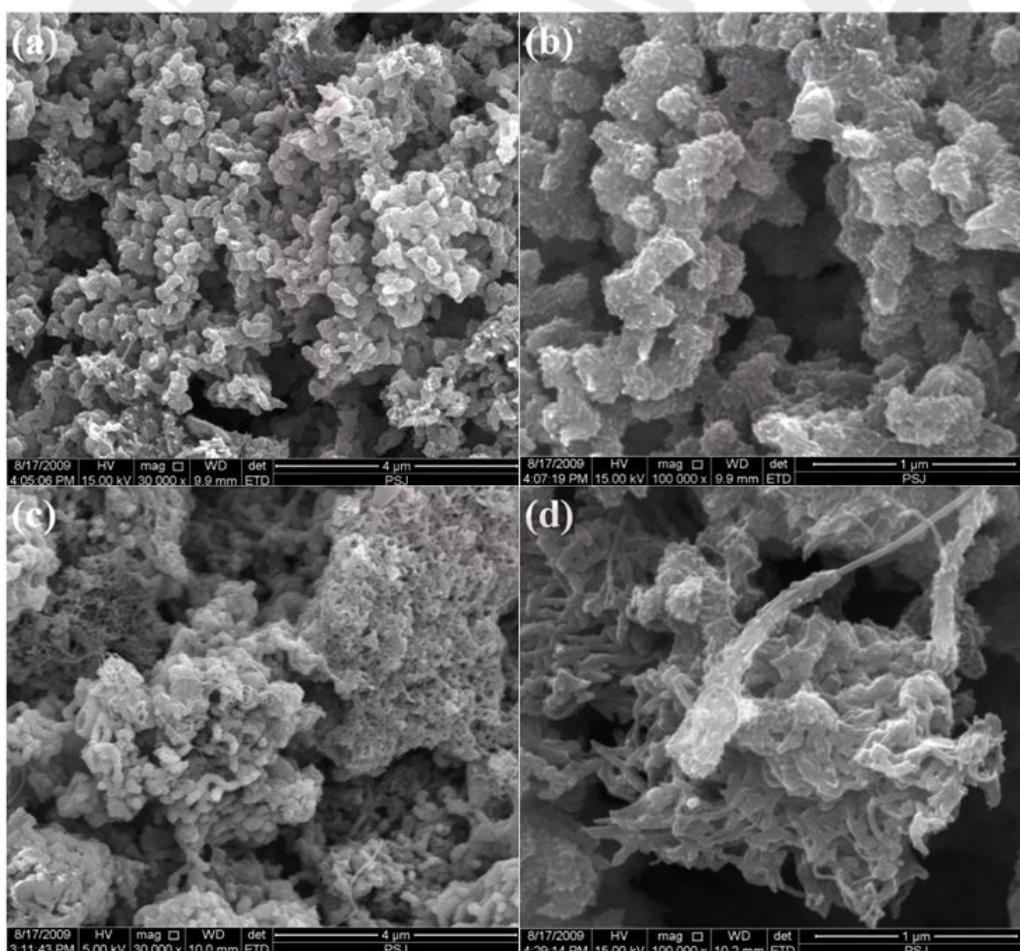


Figure 3. SEM images: (a) PANi (30,000×), (b) PANi (100,000×), (c) PANi/PANi-g-MWNT mixture (30,000×), (d) PANi/PANi-g-MWNT mixture (100,000×).

3.5 Transmission Electron Microscopy

To further assure that MWNT remained intact during the reaction and work-up procedures, and also to verify the covalent attachment of PANi onto the surface of MWNT, TEM study was conducted. For the TEM sample preparation, PANi/PANi-g-MWNT mixture was dispersed in acetone; a carbon-coated copper grid was dipped into this mixture and taken out to dry in a vacuum oven. The TEM images show that the morphology of PANi is irregular form without concentric hollow interior. (Figure 4a, b). The TEM images of PANi/PANi-g-MWNT mixture show that the surface of AF-MWNT was heavily decorated with PANi (Figure 4c, d). Furthermore, the distinct graphitic planes from the MWNT framework at higher magnification implicate that MWNT was not damaged during the grafting-polymerization reactions and work-up procedures. The unique microscopic results from SEM and TEM explained that the two reaction conditions applied in this work are indeed effective for the functionalization and grafting of MWNT. Hence, it could be concluded that PANi was efficiently grafted onto the surface of the AF-MWNT to afford PANi/PANi-g-MWNT mixture composite.

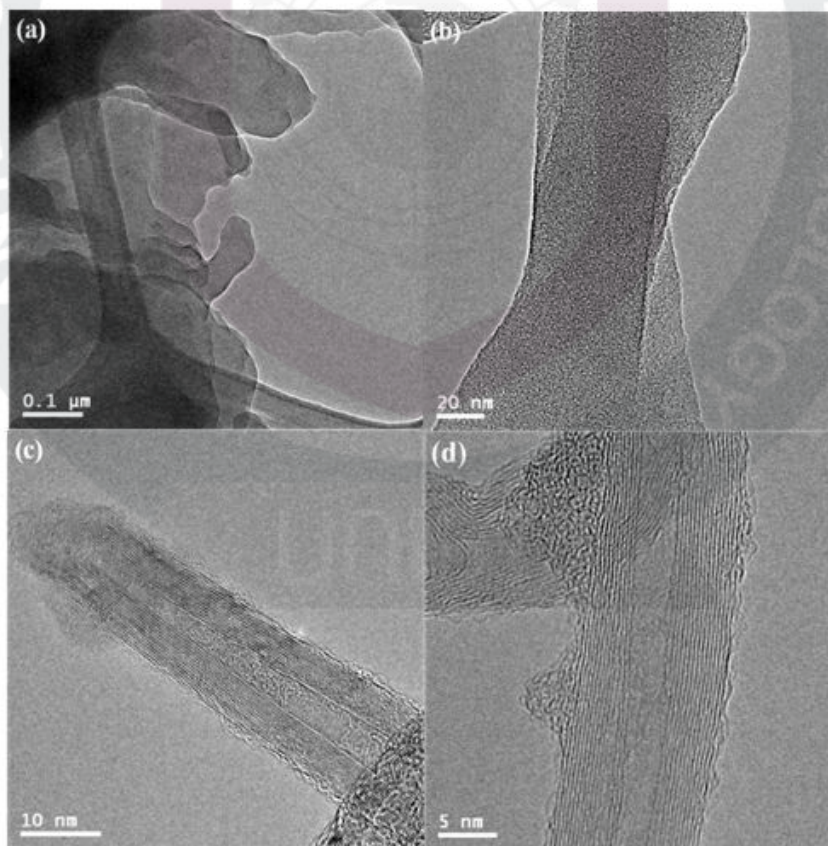


Figure 4. TEM images: (a) PANi (30,000×), (b) PANi (150,000×), (c) PANi/PANi-g-MWNT mixture (300,000×), (d) PANi/PANi-g-MWNT mixture (500,000×).

3.6 BET surface area

To measure surface area using the BET method, the PANi and PANi/PANi-g-MWNT mixture were dedoped into 1M aqueous ammonium hydroxide to minimize the effect of the dopants and then the powder samples were degassed under vacuum at 100 °C before measurement. The BET surface areas of PANi and PANi/PANi-g-MWNT mixture were 6.991 and 9.680 m²/g, respectively (Table 2). The surface area of PANi/PANi-g-MWNT mixture was almost 38 % higher than that of PANi. Because MWNT have high specific surface area.

Table 2. BET surface area, pore volume and average pore size of PANi and PANi/PANi-g-MWNT mixture.

Sample	Surface area (m ² /g)	Pore volume (ml/g)	Pore size (Å)
Dedoped PANi	6.991	0.02485	164.5
Dedoped PANi/PANi-g-MWNT mixture	9.680	0.03440	168.9

3.7 UV-vis absorption and emission behaviors.

UV-vis absorption and emission measurements were conducted to study the interfacial interaction between PANi and MWNT. Stock solution (10 mg/L) of each sample was prepared in NMP. The UV-absorption of PANi showed two peaks at 298 and 612 nm. Both peaks are related to the $\pi \rightarrow \pi^*$ transition of benzenoid ring and quinoid ring in PANi, respectively, which are identical to those of dedoped PANi.³⁰ These results agree with WAXD results that most of HCl was removed (dedoped) from both PANi and PANi/PANi-g-MWNT mixture during Soxhlet extraction. Compared to the PANi homopolymer, which showed peak maxima at 298 and 612 nm, the peaks from PANi/PANi-g-MWNT mixture showed maxima at 326 and 571 nm, respectively (Figure 5a). The first peak, which was red-shifted, implied that there was a strong interaction between PANi and MWNT. The result support that PANi is covalently grafted onto the surface of AF-MWNT.

Fluorescent measurements of the samples were conducted using the excitation wavelength of UV absorption maximum of each sample. The emission maxima of PANi and PANi/PANi-g-MWNT mixture were at 339 and 466 nm, respectively (Figure 5b). The peak maximum was 127nm red-shifted with much higher peak intensity, which could be due to the fact that PANi was uniformly grafted onto the surface of AF-MWNT and the effective conjugation length was significantly extended. A uniform covalent coating of PANi could suppress the AF-MWNT influence at excited state. If AF-MWNT and PANi were physically aggregated by intermolecular π - π interaction in solid state, and were segregated in solution, the emission intensity of PANi/PANi-g-MWNT mixture would be much higher and the peak location should be stay almost identical.

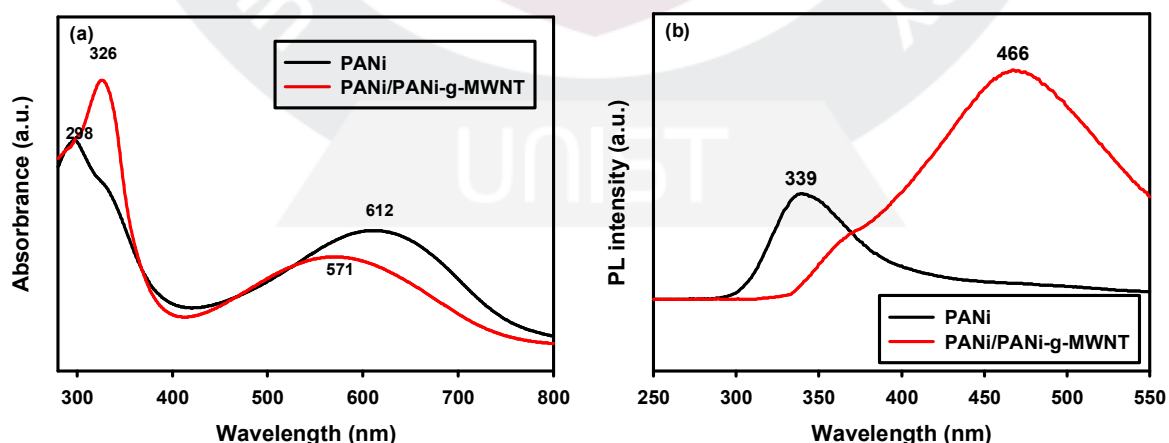


Figure 5. UV-vis absorption and emission spectra of PANi and PANi/PANi-g-MWNT mixture: (a) absorption, (b) emission.

3.8 Cyclic Voltammetry

Cyclic voltammetry (CV) has generally been used to investigate the electrochemical properties of conductive materials. PANi and PANi/PANi-g-MWNT mixture were characterized by CV using a three-electrode electrochemical cell. The 10th cyclic voltammetry curve recorded on carbon cloth coated with a PANi and PANi/PANi-g-MWNT mixture (Figure 6). Cyclic voltammetry studies were performed in aqueous solution of 0.1M H₂SO₄, in the potential range from -0.25 V to 1.25 V versus Ag/AgCl at sweep rate of 10 m V/s. The broad oxidation and reduction (redox) peaks of PANi were observed at about 0.50 and 0.48 V versus Ag/AgCl, respectively. These values are related to the redox of the PANi from emeraldine state to pernigraniline state.^{3 1}

Compare with PANi electrode, the peak currents at PANi/PANi-g-MWNT mixture electrode were increased. The peak current of the PANi/PANi-g-MWNT mixture electrode possesses higher electrocatalytic activity, resulted from its higher electroactive surface area.

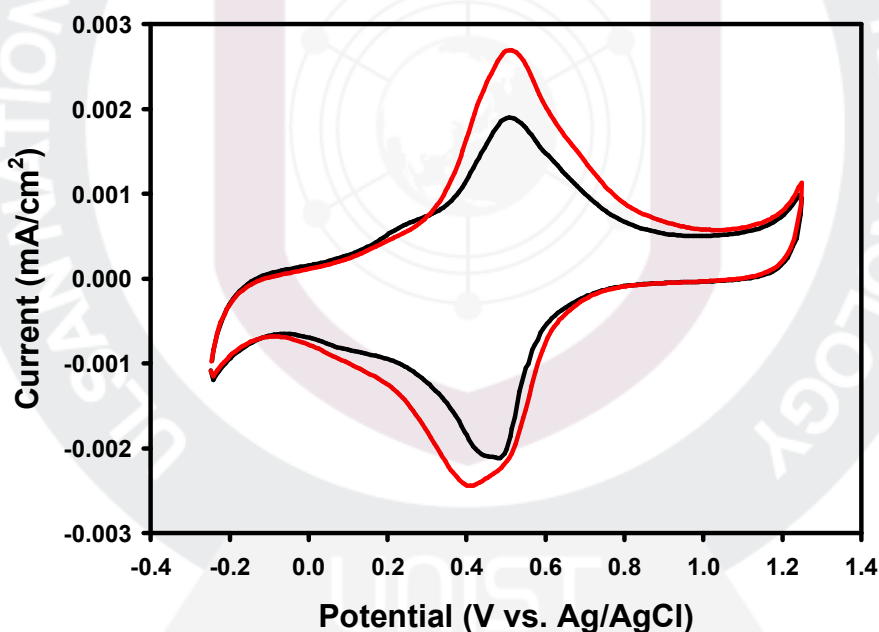


Figure 6 Cyclic voltammograms of PANi and PANi/PANi-g-MWNT mixture in 0.1M H₂SO₄ aqueous solution. Scan rate is 10mV/s (black line) PANi, (red line) PANi/PANi-g-MWNT mixture.

3.9 Electrical Characteristics

All test films were prepared by compression molding at high pressure (60MPa). The conductivity at room temperature was measured at 10 different locations and averaged. The values were determined using the following equation $\sigma = 1/(\rho \cdot cf \cdot d)$, where σ , ρ , cf and d are the conductivity, the resistivity, correction factor (4.340) and sample thickness in that order.^{3 2} The calculated conductivity of as-prepared PANi/PANi-g-MWNT was 3.65 S/cm. The value was 1.7 times higher than the value (2.12 S/cm) obtained from as-prepared PANi homopolymer (Table 3). The conductivity of PANi homopolymer after Soxhlet extraction (partially dedoped) was catastrophically dropped to 1.40×10^{-5} S/cm, while that of PANi/PANi-g-MWNT was still high at 5.17×10^{-2} S/cm. The difference was as high as ~ 3500 orders of magnitude. Both values indicate that a trace amount of HCl may still remain in the matrices and play as a dopant, because the conductivity of completely dedoped PANi is in the range of insulator (10^{-6} S/cm). However, WAXD and UV results have indicated that HCl was almost completely removed during Soxhlet extraction. After measuring the conductivities of as-prepared PANi and PANi/PANi-g-MWNT mixture, the samples were converted into the base form by treatment with 1M aqueous ammonia. As expected, the conductivity of dedoped PANi was out of detection limit (1×10^{-6} S/cm), whereas that of dedoped PANi/PANi-g-MWNT was still high at 1.36×10^{-2} S/cm. Although PANi/PANi-g-MWNT consists of PANi and PANi-g-MWNT, maintaining relatively much higher conductivity is that the portion of PANi-g-MWNT is doped by MWNT instead of HCl and MWNT plays as conducting bridge as well. The dedoped PANi and PANi/PANi-g-MWNT mixture were redoped by immersion into 1M aqueous HCl solution and dried. The redoped PANi/PANi-g-MWNT mixture displayed a good conductivity of 9.5×10^{-1} S/cm, which was in the semi-metallic region. This value was approximately 3 times higher than the conductivity of redoped PANi (3.75×10^{-1} S/cm). Thus, the conductivity of PANi was significantly improved by grafting onto the surface of MWNT. This is due to the fact that the charge transfer from electron-rich PANi to electron-deficient MWNT is quite efficient.^{3 3} Similar result was recently reported by Lee and co-workers that an in-situ nanocomposite containing 10 wt% carboxylic acid-functionalized MWNT and PANi doped with dodecyl sulfate and prepared via an emulsion polymerization of aniline showed an electrical conductivity of 2.72×10^{-1} S/cm.^{3 4}

Table 3. Conductivities of PANi and PANi/PANi-g-MWNT mixture with respect to their doping state.

State	Sample	Conductivity (S/cm)
As-prepared	PANi	2.12
	PANi/PANi-g-MWNT	3.65
After Soxhlet Extraction	PANi	1.40×10^{-5}
	PANi/PANi-g-MWNT	5.17×10^{-2}
Dedoped with 1M NH ₃ (aq.)	PANi	Out of measuring limit
	PANi/PANi-g-MWNT	1.36×10^{-2}
Redoped with 1M HCl	PANi	3.75×10^{-1}
	PANi/PANi-g-MWNT	9.5×10^{-1}

Conclusions

The MWNT was first functionalized with 4-aminobenzoic acid to afford AF-MWNT, which was subsequently grafted with PANi via suspension polymerization to generate a PANi/PANi-g-MWNT nanocomposite. The resultant composite was characterized with various analytical techniques such as FT-IR, WAXD, SEM, TEM, UV-vis and fluorescence spectroscopy. From the CV and conductivity measurements, PANi/PANi-g-MWNT composite displayed significantly improved conductivity and capacitance over PANi homopolymer. Thus, it could be concluded that the two-step reaction sequence for the Friedel-Crafts functionalization of MWNT and the subsequent grafting of PANi onto the surface of AF-MWNT were indeed a feasible approach for the hybridization of carbon-based nanomaterials and functional polymers. As a result, it is a reasonable expectation that synergistic enhancement could be obtained from the special attributes of each component, leading to the development of a new class of advanced materials for various electronic and opto-electronic applications. And also, we supposed that if hybridized material, which is made by Friedel-Crafts functionalization and grafting of polymers is combined with CNT as conductive dopants, new hybridized material will display better conductivity.

REFERENCES

- ¹ CHIANG, C. K., FINCHER, C. R., PARK, Y. W., HEEGER, A. J., SHIRAKAWA, H., LOUIS, E. J., GAU, S. C. & MACDIARMID, A. G. 1977. Electrical conductivity in doped polyacetylene. *Physical Review Letters*, 39, 1098-1101.
- ² MACDIARMID, A. G., ASTURIAS, G. S., KERSHNER, D. L., MANOHAR, S. K., RAY, A., SCHERR, E. M., SUN, Y., TANG, X. & EPSTEIN, A. J. Year. Polyanilines: processing, molecular weight, oxidation state and derivatives. *In*, 1989 Dallas, TX, USA. Publ by ACS, 147-148.
- ³ (a) LUZNY, W. & BAŇKA, E. 2000. Relations between the structure and electric conductivity of polyaniline protonated with camphorsulfonic acid. *Macromolecules*, 33, 425-429. (b) STEJSKAL, J., SAPURINA, I., TRCHOVA, M., PROKES, J., KRIVKA, I. & TOBOLKOVA, E. 1998. Solid-state protonation and electrical conductivity of polyaniline. *Macromolecules*, 31, 2218-2222. (c) MCCALL, R. P., SCHERR, E. M., MACDIARMID, A. G. & EPSTEIN, A. J. 1994. Anisotropic optical properties of an oriented-emeraldine-base polymer and an emeraldine-hydrochloride-salt polymer. *Physical Review B*, 50, 5094-5100. (d) STEJSKAL, J., KRATOCHVIL, P. & JENKINS, A. D. 1996. The formation of polyaniline and the nature of its structures. *Polymer*, 37, 367-369.
- ⁴ MACDIARMID, A., CHIANG, J., HALPERN, M., HUANG, W., MU, S., NANAXAKKARA, L., WU, S. & YANIGER, S. 1985. "Polyaniline": Interconversion of Metallic and Insulating Forms. *Molecular Crystals and Liquid Crystals*, 121, 173-180.
- ⁵ TSUTSUMI, H., YAMASHITA, S. & OISHI, T. 1997. Preparation of polyaniline-poly (p-styrenesulfonic acid) composite by post-polymerization and application as positive active material for a rechargeable lithium battery. *Journal of Applied Electrochemistry*, 27, 477-481.
- ⁶ PAUL, E. W., RICCO, A. J. & WRIGHTON, M. S. 1985. Resistance of polyaniline films as a function of electrochemical potential and the fabrication of polyaniline-based microelectronic devices. *Journal of Physical Chemistry*, 89, 1441-1447.
- ⁷ LEE, Y. H., KIM, C. A., JANG, W. H., CHOI, H. J. & JHON, M. S. 2001. Synthesis and electrorheological characteristics of microencapsulated polyaniline particles with melamine-formaldehyde resins. *Polymer*, 42, 8277-8283.

-
- ⁸ (a) SANGODKAR, H., SUKEERTHI, S., SRINIVASA, R. S., LAL, R. & CONTRACTOR, A. Q. 1996. A biosensor array based on polyaniline. *Analytical Chemistry*, 68, 779-783. (b) BOSSI, A., PILETSKY, S. A., PILETSKA, E. V., RIGHETTI, P. G. & TURNER, A. P. F. 2000. An assay for ascorbic acid based on polyaniline-coated microplates. *Analytical Chemistry*, 72, 4296-4300.
- ⁹ HUANG, S. C., BALL, I. J. & KANER, R. B. 1998. Polyaniline membranes for pervaporation of carboxylic acids and water. *Macromolecules*, 31, 5456-5464.
- ¹⁰ TRIVEDI, D. C. & DHAWAN, S. K. 1992. Grafting of electronically conducting polyaniline on insulating surfaces. *Journal of Materials Chemistry*, 2, 1091-1096.
- ¹¹ (a) TASIS, D., TAGMATARCHIS, N., BIANCO, A. & PRATO, M. 2006. Chemistry of carbon nanotubes. *Chemical Reviews*, 106, 1105-1136. (b) GROSSIORD, N., LOOS, J., REGEV, O. & KONING, C. E. 2006. Toolbox for dispersing carbon nanotubes into polymers to get conductive nanocomposites. *Chemistry of Materials*, 18, 1089-1099. (c) BALASUBRAMANIAN, K. & BURGHARD, M. 2005. Chemically functionalized carbon nanotubes. *Small*, 1, 180-192. (d) BANERJEE, S., KAHN, M. G. C. & WONG, S. S. 2003. Rational chemical strategies for carbon nanotube functionalization. *Chemistry - A European Journal*, 9, 1898-1908.
- ¹² (a) PRADHAN, B., SETYOWATI, K., LIU, H., WALDECK, D. H. & CHEN, J. 2008. Carbon nanotube-polymer nanocomposite infrared sensor. *Nano Letters*, 8, 1142-1146. (b) WANG, F., GU, H. & SWAGER, T. M. 2008. Carbon nanotube/polythiophene chemiresistive sensors for chemical warfare agents. *Journal of the American Chemical Society*, 130, 5392-5393. (c) WEI, C., DAI, L., ROY, A. & TOLLE, T. B. 2006. Multifunctional chemical vapor sensors of aligned carbon nanotube and polymer composites. *Journal of the American Chemical Society*, 128, 1412-1413. (d) WU, T. M. & LIN, Y. W. 2006. Doped polyaniline/multi-walled carbon nanotube composites: Preparation, characterization and properties. *Polymer*, 47, 3576-3582.
- ¹³ ZENGİN, H., ZHOU, W., JIN, J., CZERW, R., SMITH JR, D. W., ECHEGOYEN, L., CARROLL, D. L., FOULGER, S. H. & BALLATO, J. 2002. Carbon nanotube doped polyaniline. *Advanced Materials*, 14, 1480-1483.
- ¹⁴ WOO, H. S., CZERW, R., WEBSTER, S., CARROLL, D. L., PARK, J. W. & LEE, J. H. 2001.

Organic light emitting diodes fabricated with single wall carbon nanotubes dispersed in a hole conducting buffer: The role of carbon nanotubes in a hole conducting polymer. *Synthetic Metals*, 116, 369-372.

- ^{1 5} KYMAKIS, E. & AMARATUNGA, G. A. J. 2002. Single-wall carbon nanotube/conjugated polymer photovoltaic devices. *Applied Physics Letters*, 80, 112.
- ^{1 6} AGO, H., PETRITSCH, K., SHAFFER, M. S. P., WINDLE, A. H. & FRIEND, R. H. 1999. Composites of carbon nanotubes and conjugated polymers for photovoltaic devices. *Advanced Materials*, 11, 1281-1285.
- ^{1 7} CHENG, G., ZHAO, J., TU, Y., HE, P. & FANG, Y. 2005. A sensitive DNA electrochemical biosensor based on magnetite with a glassy carbon electrode modified by multi-walled carbon nanotubes in polypyrrole. *Analytica Chimica Acta*, 533, 11-16.
- ^{1 8} QU, F., YANG, M., JIANG, J., SHEN, G. & YU, R. 2005. Amperometric biosensor for chorine based on layer-by-layer assembled functionalized carbon nanotube and polyaniline multilayer film. *Analytical Biochemistry*, 344, 108-114.
- ^{1 9} AN, K. H., JEONG, S. Y., HWANG, H. R. & LEE, Y. H. 2004. Enhanced sensitivity of a gas sensor incorporating single-walled carbon nanotube-polypyrrole nanocomposites. *Advanced Materials*, 16, 1005-1009.
- ^{2 0} LEFENFELD, M., BLANCHET, G. & ROGERS, J. A. 2003. High-performance contacts in plastic transistors and logic gates that use printed electrodes of DNNSA-PANI doped with single-walled carbon nanotubes. *Advanced Materials*, 15, 1188-1191.
- ^{2 1} (a) ALI, S. R., MA, Y., PARAJULI, R. R., BALOGUN, Y., LAI, W. Y. C. & HE, H. 2007. A nonoxidative sensor based on a self-doped polyaniline/carbon nanotube composite for sensitive and selective detection of the neurotransmitter dopamine. *Analytical Chemistry*, 79, 2583-2587. (b) GUO, L. & PENG, Z. 2008. One-pot synthesis of carbon nanotube-polyaniline-gold nanoparticle and carbon nanotube-gold nanoparticle composites by using aromatic amine chemistry. *Langmuir*, 24, 8971-8975. (c) LIU, J., TIAN, S. & KNOLL, W. 2005. Properties of polyaniline/carbon nanotube multilayer films in neutral solution and their application for stable low-potential detection

-
- of reduced β -nicotinamide adenine dinucleotide. *Langmuir*, 21, 5596-5599. (d) PANHUIS, M. I. H., DOHERTY, K. J., SAINZ, R., BENITO, A. M. & MASER, W. K. 2008. Carbon nanotube mediated reduction in optical activity in polyaniline composite materials. *Journal of Physical Chemistry C*, 112, 1441-1445. (e) SAINZ, R., SMALL, W. R., YOUNG, N. A., VALL S, C., BENITO, A. M., MASER, W. K. & PANHUIS, M. I. H. 2006. Synthesis and properties of optically active polyaniline carbon nanotube composites. *Macromolecules*, 39, 7324-7332. (f) YAN, X. B., HAN, Z. J., YANG, Y. & TAY, B. K. 2007. Fabrication of carbon nanotube-polyaniline composites via electrostatic adsorption in aqueous colloids. *Journal of Physical Chemistry C*, 111, 4125-4131.
- ^{2 2} (a) CHEN, J., RAO, A. M., LYUKSYUTOV, S., ITKIS, M. E., HAMON, M. A., HU, H., COHN, R. W., EKLUND, P. C., COLBERT, D. T., SMALLEY, R. E. & HADDON, R. C. 2001. Dissolution of full-length single-walled carbon nanotubes. *Journal of Physical Chemistry B*, 105, 2525-2528. (b) RAMESH, S., ERICSON, L. M., DAVIS, V. A., SAINI, R. K., KITTRELL, C., PASQUALI, M., BILLUPS, W. E., ADAMS, W. W., HAUGE, R. H. & SMALLEY, R. E. 2004. Dissolution of pristine single walled carbon nanotubes in superacids by direct protonation. *Journal of Physical Chemistry B*, 108, 8794-8798.
- ^{2 3} (a) MONTHIOUX, M., SMITH, B. W., BURTEAUX, B., CLAYE, A., FISCHER, J. E. & LUZZI, D. E. 2001. Sensitivity of single-wall carbon nanotubes to chemical processing: An electron microscopy investigation. *Carbon*, 39, 1251-1272. (b) SALZMANN, C. G., LLEWELLYN, S. A., TOBIAS, G., WARD, M. A. H., HUH, Y. & GREEN, M. L. H. 2007. The role of carboxylated carbonaceous fragments in the functionalization and spectroscopy of a single-walled carbon-nanotube material. *Advanced Materials*, 19, 883-887. (c) ZHANG, Y., SHI, Z., GU, Z. & IJIMA, S. 2000. Structure modification of single-wall carbon nanotubes. *Carbon*, 38, 2055-2059.
- ^{2 4} SAMMALKORPI, M., KRASHENINNIKOV, A., KURONEN, A., NORDLUND, K. & KASKI, K. 2004. Mechanical properties of carbon nanotubes with vacancies and related defects. *Physical Review B - Condensed Matter and Materials Physics*, 70, 1-8.
- ^{2 5} (a) BAEK, J. B., LYONS, C. B. & TAN, L. S. 2004. Covalent modification of vapour-grown carbon nanofibers via direct Friedel-Crafts acylation in polyphosphoric acid. *Journal of Materials Chemistry*, 14, 2052-2056. (b) JEONG, J. Y., LEE, H. J., KANG, S. W., TAN, L. S. & BAEK, J. B. 2008. Nylon 610/functionalized multiwalled carbon nanotube composite prepared from in-situ interfacial polymerization. *Journal of Polymer Science, Part A: Polymer Chemistry*, 46, 6041-6050.

-
- (c) JEON, I. Y., TAN, L. S. & BAEK, J. B. 2008. Nanocomposites derived from in situ grafting of linear and hyperbranched poly(ether-ketone)s containing flexible oxyethylene spacers onto the surface of multiwalled carbon nanotubes. *Journal of Polymer Science, Part A: Polymer Chemistry*, 46, 3471-3481.
- ^{2 6} JEON, I. Y., LEE, H. J., CHOI, Y. S., TAN, L. S. & BAEK, J. B. 2008. Semimetallic transport in nanocomposites derived from grafting of linear and hyperbranched poly (phenylene sulfide)s onto the surface of functionalized multi-walled carbon nanotubes. *Macromolecules*, 41, 7423-7432.
- ^{2 7} (a) BAEK, J. B. & TAN, L. S. 2003. Improved syntheses of poly (oxy-1,3-phenylenecarbonyl-1,4-phenylene) and related poly(ether-ketones) using polyphosphoric acid/P₂O₅ as polymerization medium. *Polymer*, 44, 4135-4147. (b) HAN, S. W., OH, S. J., TAN, L. S. & BAEK, J. B. 2008. One-pot purification and functionalization of single-walled carbon nanotubes in less-corrosive poly(phosphoric acid). *Carbon*, 46, 1841-1849. (c) LEE, H. J., HAN, S. W., KWON, Y. D., TAN, L. S. & BAEK, J. B. 2008. Functionalization of multi-walled carbon nanotubes with various 4-substituted benzoic acids in mild polyphosphoric acid/phosphorous pentoxide. *Carbon*, 46, 1850-1859.
- ^{2 8} ŁUZNY, W., ŚNIECHOWSKI, M. & LASKA, J. 2002. Structural properties of emeraldine base and the role of water contents: X-ray diffraction and computer modelling study. *Synthetic Metals*, 126, 27-35.
- ^{2 9} JEON, I. Y., LOON-SENG, T. A. N. & BAEK, J. B. 2010. Synthesis and electrical properties of polyaniline/polyaniline grafted multiwalled carbon nanotube mixture via in situ static interfacial polymerization. *Journal of Polymer Science, Part A: Polymer Chemistry*, 48, 1962-1972.
- ^{3 0} LI, G., JIANG, L. & PENG, H. 2007. One-dimensional polyaniline nanostructures with controllable surfaces and diameters using vanadic acid as the oxidant. *Macromolecules*, 40, 7890-7894.
- ^{3 1} (a) CHEN, R. & BENICEWICZ, B. C. 2003. Preparation and properties of poly(methacrylamide)s containing oligoaniline side chains. *Macromolecules*, 36, 6333-6339. (b) SINGER, R. A., SADIGHI, J. P. & BUCHWALD, S. L. 1998. A general synthesis of end-functionalized oligoanilines via palladium-catalyzed amination. *Journal of the American Chemical Society*, 120, 213-214.
- ^{3 2} PERLOFF, D. S. 1977. Four-point sheet resistance correction factors for thin rectangular samples.

Solid State Electronics, 20, 681-687.

- ^{3 3} WU, T. M., LIN, Y. W. & LIAO, C. S. 2005. Preparation and characterization of polyaniline/multi-walled carbon nanotube composites. *Carbon*, 43, 734-740.
- ^{3 4} JEEVANANDA, T., SIDDARAMAIAH, KIM, N. H., HEO, S. B. & LEE, J. H. 2008. Synthesis and characterization of polyaniline-multiwalled carbon nanotube nanocomposites in the presence of sodium dodecyl sulfate. *Polymers for Advanced Technologies*, 19, 1754-1762.



Appendix

The functionalization of MWNT was conveniently monitored by FT-IR (Figure S1). Pristine MWNT displayed featureless FTIR spectrum at normal magnification. However, in the zoomed-in region of the spectra, there are sp^2 C-H and sp^3 C-H stretching bands at 2924cm^{-1} (Figure S1, inset). The peak is attributed by the defects at side walls and open ends of MWNTs. These defects should be originated from the synthetic process of MWNT with hydrocarbon feedstock. AF-MWNT clearly showed an aromatic carbonyl (C=O) peak at 1644cm^{-1} of carboxylic acid in 4-aminobenzoic acid.

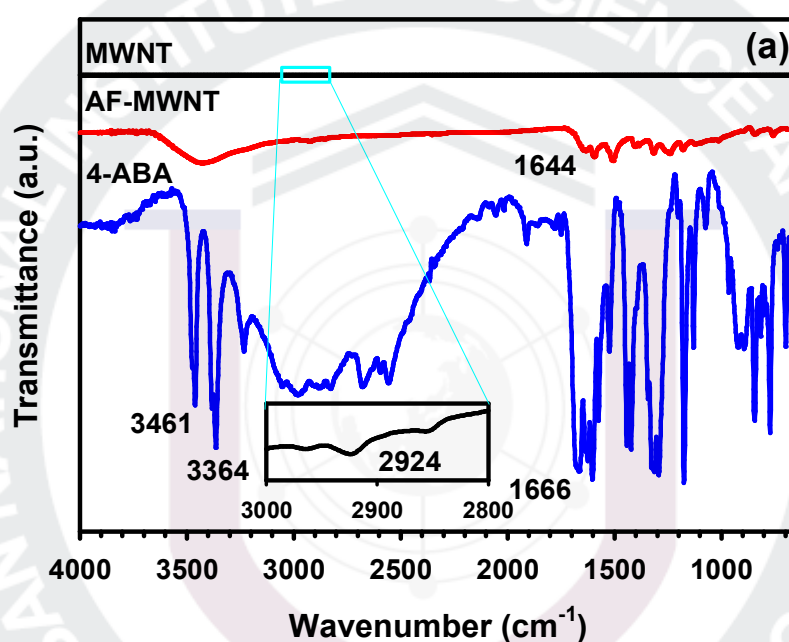


Figure S1. FT-IR (KBr pellet) spectra of as-received MWNT, AF-MWNT and 4-aminobenzoic acid

The functionalization of MWNT as further confirmed by SEM imaging. Pristine MWNT shows that the tubes have seamless and smooth surfaces with the average diameter of 10~20nm (Figure S2(a)). Thus, the average diameter of AF-MWNT is increased to ~40~50nm (Figure S2(b)). Considering the length of 4-aminobenzoyl moiety, which is ~1nm, the average diameter of AF-MWNT should be in the range of 12~22nm. The unexpected larger diameter is likely due to the bundling of polar AF-MWNT. The driving force for bundling of polar surface groups of functionalized MWNT could stem from stronger epitaxial interaction is strong enough to overcome the structural rigidity, MWNT is forced to bundle along the lateral surface. Specifically, AF-MWNT are able to form strong hydrogen bonding. Fortuitously, the average diameter dimension of bundled AF-MWNT in the SEM image is ~40~50nm, which agreed well with the diameter of a bundle containing four AF-MWNT. (Figure S2(b)). TEM grid was dipped into the dilute solution and vacuum dried, and with it were obtained TEM images, which clearly showed individual tubes with diameter dimension of 20nm (Figure S2 (c,d)).

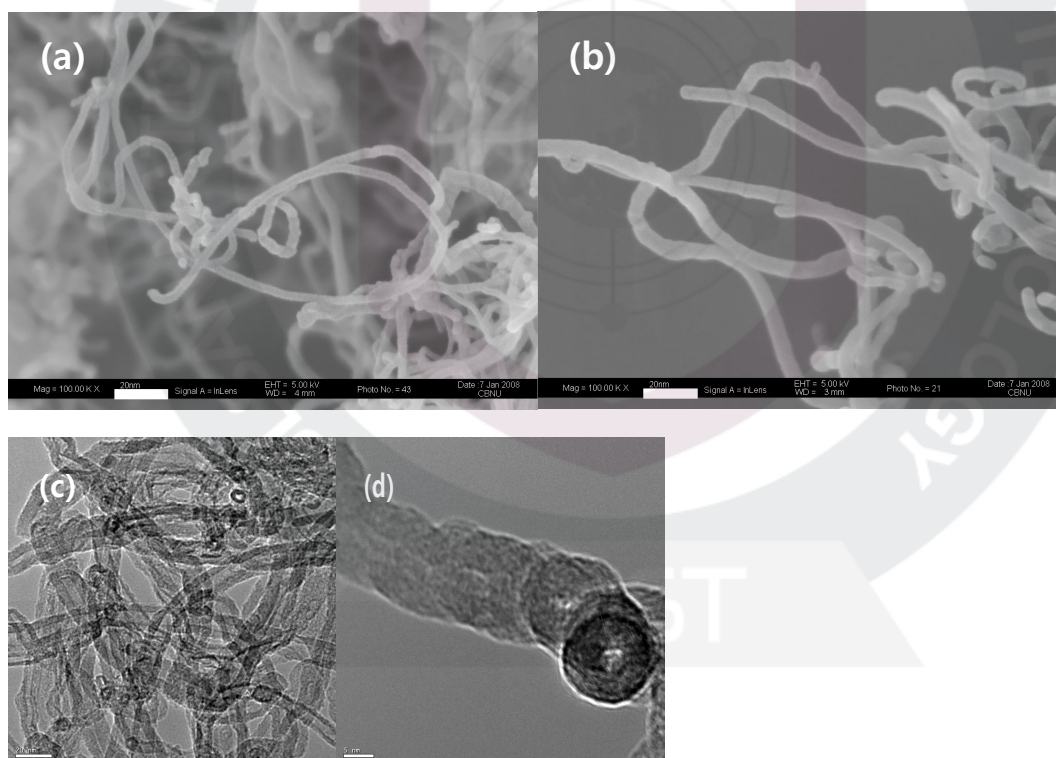


Figure S2. (a) SEM image of as-received MWNT (100,000 \times , scale bar is 100 nm), (b) SEM image of AF-MWNT (100,000 \times , scale bar is 100 nm), (c) TEM image of AF-MWNT at lower magnification (scale bar is 20 nm), (d) TEM image of AF-MWNT at higher magnification (scale bar is 5 nm).

To determine the amount of 4-aminobenzoyl moiety, the powder samples were subjected to thermogravimetric analysis (TGA). The weight loss of AF-MWNT was ~48% around 660 °C, at which the two curves from pristine MWNT and AF-MWNT crossed (Figure S3). The weight loss was attributed to thermally stripping off of 4-aminobenzoyl moieties was covalently attached to the surface of AF-MWNT. Interestingly, the thermo-oxidative stability of AF-MWNT above 660 °C is higher than pristine MWNT.

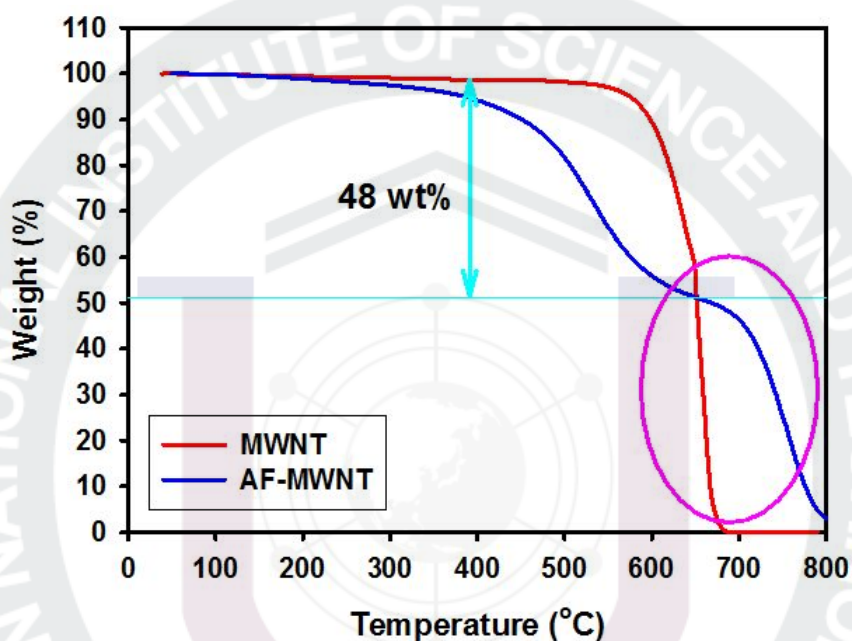


Figure S3. TGA image of MWNT and AF-MWNT in air with heating rate of 10 °C /min, showing that 48 wt% of 4-aminobenzoyl (AF-) moiety is grafted on the surface of MWNT.

Manuscript

Journal

JEON, I. Y., Kang, S. W., TAN, L. S. & BAEK, J. B. 2010. Grafting of Polyaniline onto the surface of 4-Aminobenzoyl-Functionalized Multiwalled Carbon Nanotube and Its Electrochemical Properties *Journal of Polymer Science, Part A: Polymer Chemistry*, 48, 3103-3112.

Proceeding

International

"Electrochemical properties of polyaniline doped by carboxylic acid or sulfonic acid-terminated hyperbranched poly(ether-ketone)s" Polym. Prepr. 2009, 49(2), Salt Lake, UT, March 22-26.

Domestic

"Synthesis and Characterization of Star-Shaped Polyurethane using a Novel Hyperbranched Polyester Polyol Core" The Polymer Society of Korea 2008, 33(1) (Daejeon, April 11-12).

"Doping of Conducting Polymer by Hyperbranched Polymer" The Polymer Society of Korea 2008, 33(2). (KINTEX, Ilsan, October 9-10, 2008).

"Electrochemical properties of polyaniline doped by carboxylic acid or sulfonic acid-terminated hyperbranched poly(ether-ketone)s" The Polymer Society of Korea 2009, 34(1) (Daejeon, April 9-10).

"In-situ synthesis of polymeric acids doped polyaniline via oxidative polymerization" The polymer Society of Korea 2009, 34(2), (Gwangju, October 8-9).

"Polyaniline doped by hyperbranched poly(ether-ketone)s" The polymer Society of Korea 2010, 35(1), (Daejeon, April 8-9).

Acknowledgements

I am very pleased to finish my thesis at UNIST. Throughout my years at graduate school in UNIST, I truly learned a lot, especially from this thesis work. First and foremost, I would like to thank my parents, for giving me strength and courage to do this work. I would also like to thank Professor Jong-Beom Baek, my supervisor for not only giving me the opportunity to work as his student but also being a great mentor. I am grateful to Ph.D. Dong-Wook Jang and master In-Yup Jeon for his guidance.

I would like to thank my parents and grandparents for their love and continuous support through prayers and encouragements. They were always good role models to me. I also thank my brother.

I am particularly grateful to JongKwan, JiYe and HyunJung. As master's degree students in the last semester, we spent most of our days working on thesis together at the lab. They formed the core of my research time and have been crucial to my graduate school years. I ran into good luck when I met you.

I am also grateful to my friends JongJin, Jason, SangWoo, SangHun, KyungSu, JungIl, SeungWon and junior students SeoYoon, Yeonran, GyoungJu, GyoungSik, YoungSim, MyoungHee, MiHee whose encouragements were invaluable throughout my years at UNIST.

